Cytometry 21:187–196 (1995)

Heterogeneous Calcium Flux in Peripheral T Cell Subsets Revealed by Five-Color Flow Cytometry Using Log-Ratio Circuitry

M. Roederer, M. Bigos, T. Nozaki, R.T. Stovel, D.R. Parks, and L.A. Herzenberg
Department of Genetics, Stanford University School of Medicine, Stanford, California

Received for publication October 13, 1994; accepted April 8, 1995

Calcium flux measurements of different subpopulations of cells by flow cytometry are important in understanding complex interactions in the immune system. This paper discusses the use of the difference of Log signals as a preferred method for obtaining this information simultaneously with other immunofluorescence parameters. We describe simple modifications to a commercial instrument that enables the measurement of calcium flux in addition to three immunofluorescence parameters. Finally, we show an application of this technique to measuring calcium flux of T cell subsets in human blood. We show that different subsets of peripheral CD4 T cells have significantly different capabilities to flux calcium after CD3 stimulation. These differences are related to the functional capacities of the cells within these subsets.

Key terms: T cell subsets, calcium flux, T cell function, multiparameter measurements, logarithmic amplification

In flow cytometry, many applications require the processing of the raw analog peak-height measurements to obtain useful results. For example, in many immunofluorescence applications, linear recombination of various signals is required to obtain individual reagent measurements (3). This is commonly known as fluorescence compensation. Another example is the use of metachromatic dyes. These dyes generally measure physiologic properties of cells by having emission spectra that change in response to differences in (for instance) ion concentrations. Thus, their emission spectrum depends upon some cellular state, which may vary over time or from cell to cell. The flow instrument measures the emissions of metachromatic dyes at two different selected wavelength bands; the desired parameter for data analysis is the ratio of these two signals. A difference in this ratio either between different cells or over time will directly reflect varying physiological properties.

A ratio is a synthetic measurement derived from two primary signals. To be fully functional, such a synthesis needs to provide the following two capabilities: First, a real-time display (e.g., a histogram) of the ratio signal is very useful for monitoring; otherwise, the only visual feedback the user will have concerning the integrity of data samples being run is a display of the primary signals. Second is the ability to sort cells based on the ratio. Although flow analysis has provided the answer to many biological questions, sorting is an integral part of the flow paradigm and should not be compromised. Moreover, the design of a method of synthesizing a ratio must also address questions of scaling and dynamic range of the primary signals and the resultant ratio. Because a ratio is the quotient of two values, its potential magnitude may be quite different than that of either primary signal. Finally, the actual calculation method itself may accept inputs only within a certain range of values.

The method of synthesis can be either in electronic hardware or in computer software or a hybrid of both. This paper will focus on solutions using electronic hardware, because the vast majority of cytometers currently functioning calculate ratios using electronic hardware, and our proposed logarithmic (Log)-ratio approach is hardware based. Moreover, many of the details involved in a software ratio are fundamentally different and, we believe, can best be addressed in a separate discussion. This should not be taken to imply that we are opposed to or have questions regarding the feasibility of software ratios. On the contrary, we believe that, in the not-too-distant future, most flow instruments will incorporate real-time software, including ratios, as part of their design.

The current commercial cytometers from both major manufacturers (Becton Dickinson Immunocytometry

Part of this work was presented as a poster at ISAC XV Congress, Bergen, Norway, August 25–30, 1991.

This research was supported by NIH grants AI-31770, CA-42509, and LM-04836. Address reprint requests to M. Roederer, Department of Genetics, Beckman Center B011, Stanford University, Stanford, CA 94305-5125.

Systems, San Jose, CA; Coulter Corporation, Hialeah, FL) use integrated circuits to compute analog ratios by division of the linear input signals. This method uses analog multiplier circuitry operating on signals obtained after preamplification. The ratio circuit output is then amplified, the peak is detected, and the output is digitized in a manner very similar to the raw analog signals. Because the preamplification is linear, in this paper we will refer to these methods as linear (Lin) ratios.

We can see from the basic design of the Lin ratio approach that there will be problems with scaling; that is, it will be difficult to visualize both small and large ratio signals on the same output scale. Moreover, our investigation of the Becton Dickinson FacstarPlus demonstrates that this implementation of the analog ratio circuitry yields valid ratios for only a very limited array of primary signal levels. Because of the fairly broad range of input signal levels that may be observed for cells in a single sample and the possibly varying levels of dye loading in different cell samples, there may be no consistent configuration [photomultiplier (PMT) voltages and gains for the primary signals and computed ratio amplifier gain] that provides satisfactory ratio measurements in a variety of experiments with differing sample intensities. We have not investigated Coulter instruments in detail; however, because of the similarity of the underlying ratio circuitry, we expect that similar results would be obtained.

To overcome these limitations of output scaling and input-signal dynamic range while preserving real-time monitoring and sorting capabilities, we have developed circuitry to generate the log of the ratio as the difference of the log-amplified signals (i.e., the log of the ratio of two signals is equal to the difference of the log of each signal). Because analog subtraction is easier to implement than analog division, and because logarithmic presentation can handle a much wider dynamic range than linear presentation, this methodology overcomes many of the limitations of Lin ratios. We call this approach Log ratios and will show that it yields more than 2 decades of usable ratio range and allows a wide range of source signal levels to be used in forming the ratio. Moreover, because our implementation of Log ratios is calculated in real time, both monitoring and sorting on the ratio measurement can be utilized.

Log ratios have been previously utilized by Rabinovitch et al. (10) on an Ortho Cytofluorograph 50HH (Ortho Diagnostic Systems, Westwood, MA) to demonstrate that the ratio of the Indo-1 violet and green signals remained constant for resting cells despite different loading concentrations of the dye. The dynamic range of their signals varied over more than 3 decades for a 0–30 μM range of dye concentration. If the authors had used their linear scale of 0–200 and had been able to place all of the brightest signals on scale, then the dimmest cells would have had a channel peak value of less than 1, which would be unsuitable for ratio calculation. Moreover, they did not demonstrate that their implementation was appropriate for sorting or real-time monitoring.

A common application of signal ratios is for the measurement of intracellular calcium concentrations using the fluorescent dye Indo-1 (12). The ratio of the violet to the blue-green fluorescence emission of this dye correlates (nonlinearly) with free cytoplasmic Ca^{2+}. The changes in calcium concentration after stimulation of T cells is an important indicator of their functional capacity. Of primary interest is the different functional capacities of T cell subsets in vivo. These subsets can be identified on the basis of differential surface antigen expression within both CD4 and CD8 lineages. These subsets have unique functional capacities, including the division between "memory" and "naive" cells. Phenotypic identification of naive and memory subsets requires, at a minimum, the simultaneous measurement of three different antigens: CD4 (or CD8), CD45RA, and CD62L (or CD11a) (6,8). We have begun to explore the functional capacities of these subsets by measuring the calcium flux after stimulation of the CD3 receptor.

Measurement of the calcium flux in these subpopulations requires the simultaneous measurement of five fluorescences: two from ultraviolet (UV) excitation to calculate the Indo-1 ratio and three from the 488 nm excitation to measure fluorescein, phycoerythrin (PE), and the Cy5-PE tandem dye. In this report, we demonstrate how to accomplish this with only minor modifications to a commercial FacstarPlus.

MATERIALS AND METHODS

Cytometry Hardware

A FacstarPlus cell sorter (Becton Dickinson) was equipped with the manufacturer's Pulse Processor Board and FL3(1) optics upgrade (providing a third fluorescence channel for the first laser). Figure 1 shows the layout of the optical bench and filters. An Innova 300 (Coherent Laser, Palo Alto, CA) running at 150 mW of 488 nm output provided excitation for measurement of forward scatter and three immunofluorescences. An Innova 90 running at 50 mW output in multiline 351–363 nm mode provided excitation in the UV for Indo-1 measurement.

Figure 2 shows the cabling configuration used to measure Log ratios. The valid threshold timing signal and held peak signals for the two channels used to form the ratio were tapped in the FacstarPlus electronics and were supplied to the Log-ratio electronics. Our current computer interface supports only eight parameters, so the Log ratio was processed in the electronic channel which is otherwise used for orthogonal light scatter (SSC). The other parameters in the configuration for this experiment are forward scatter, three visible fluorescences, two UV fluorescences, and time. An analog ramp signal externally generates the time parameter, which is fed into the digitizing electronics.

Nine-bit list-mode data were collected and analyzed using FACS/Desk software (4). Statistics are calculated on the full nine bits of data and are reported on a 0–250 scale. Kinetics data were analyzed using a modified version of KINPRO (written by M.R.). The log amplifiers on this instrument are adjusted for a nominal 3.75 decades in

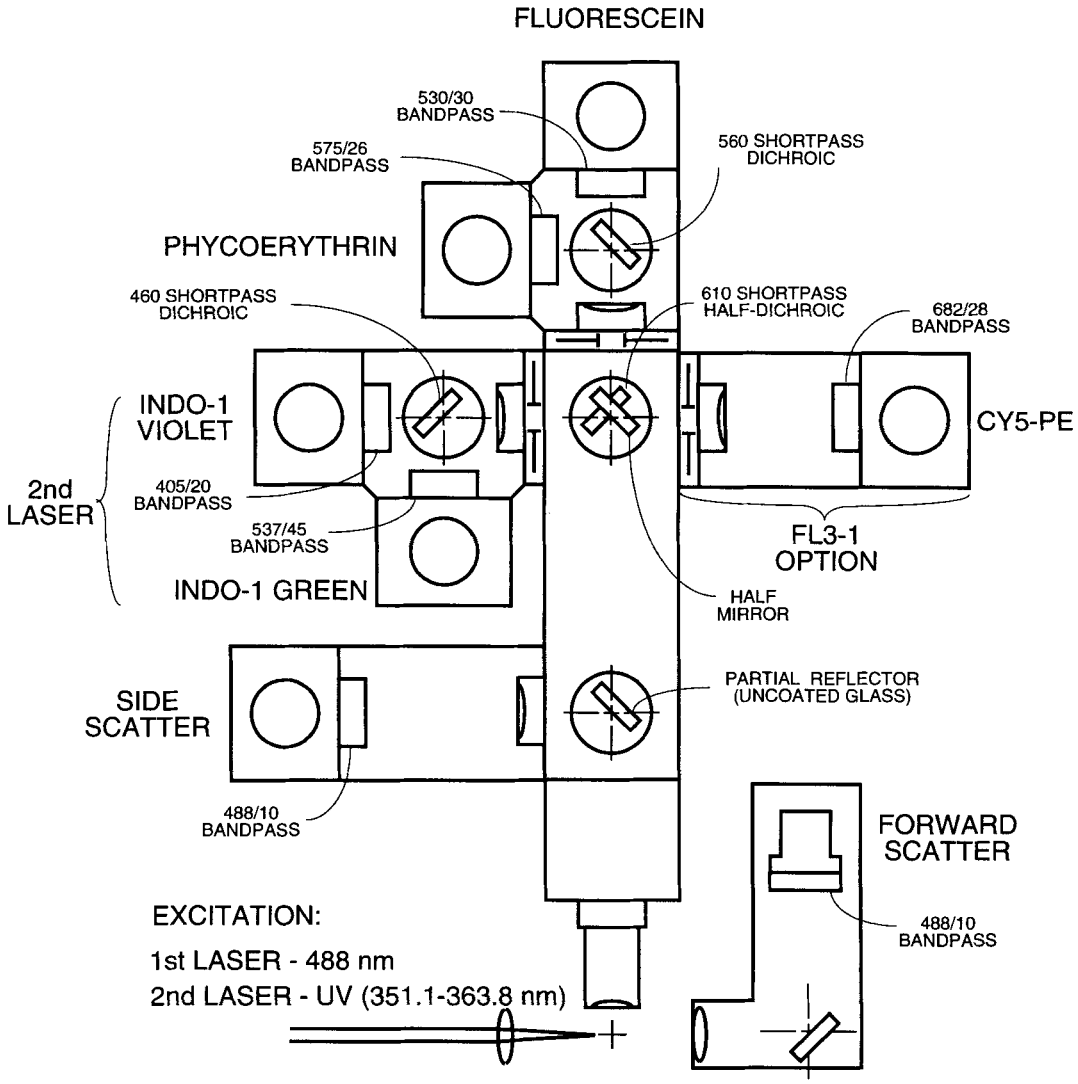

FIG. 1. Optical bench configuration for five-color/calcium. The FacstarPlus optical bench is configured with the standard Becton Dickinson FL3(1) upgrade option. The optical filters were all produced by OmegaOptical (Brattleboro, VT). A separate power supply external to the FacstarPlus (Power Designs Pacific, Inc., Palo Alto, CA) is used for the FL3(1) detector to avoid moving the side-scatter PMT cable.

250 channels, which are used for all of the following references to log channel numbers. Thus, a change of one channel (from among 250) represents (nominally) a 3.5% change in signal level.

Manufacturer's software for the FacstarPlus does not currently support the internal register settings needed for the above-described configuration. Custom software for setting the internal registers was written under a nondisclosure agreement with the manufacturer. VAX executable code is available for academic use upon request.

Figure 3 shows a block diagram of the Log-ratio circuit (a complete schematic is available upon request). The timing of the output pulse is adjusted to occur just after the peaks of the Indo-1-derived signals. This ratio pulse feeds the SSC amplifier to produce a signal that is available for monitoring on real-time dotplots or sorting. Second laser timing is set on the SSC channel, and the second laser analysis acceptance window is extended by a few microseconds to accommodate this signal. The gains of the input and output amplifiers of the Log-ratio circuit were adjusted so that equal source signal produced a midscale signal output. For Lin ratios, the Pulse Processor was calibrated and configured according to the manufacturer's guidelines (1).

Calibration particles (Rainbow Beads; Spherotech, Libertyville IL) were used to evaluate the valid input signal levels and usable dynamic range of both the pulse-processor Lin ratio and Log ratio. The beads were gated on forward scatter, so that only single particles were used for subsequent analyses. For both measurement systems, the

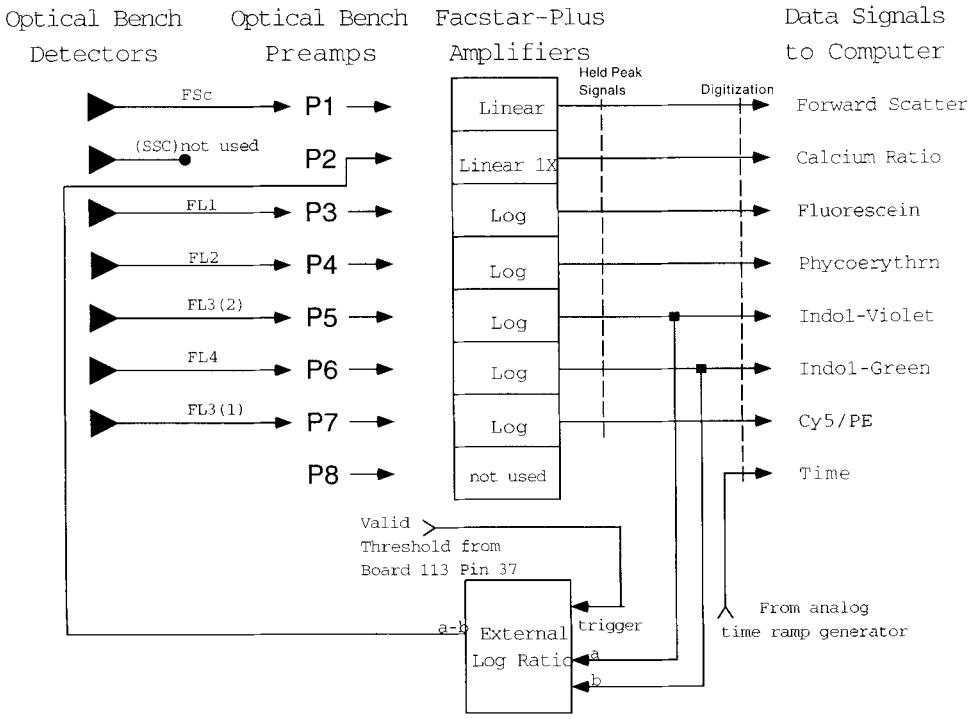

FIG. 2. Electronics configuration for five-color/calcium. The inputs to the logarithmic (Log)-ratio circuit are obtained from the FacstarPlus as follows: The Log Indo 1-violet- and Indo 1-green-held signals are obtained from the backplane test points 12 and 13, respectively. The valid threshold timing signal is obtained from board 113, pin 37. The output of the Log-ratio circuit is fed to the P2 input to the FacstarPlus electronics (normally used for side scatter); the amplifier on that channel is set to linear gain (×1). Because the Indo signals have second laser timing, the Log-ratio circuit output is also adjusted for second laser timing, and the P2 electronics are configured by software with second laser timing. The eighth parameter sent to the digitizer is the output of an analog-time ramp generator with a selectable full-scale time of 7, 14, or 21 min.

PMT voltages were initially set to give midscale ratio values. Then, the PMT voltages of the numerator and denominator channels were independently adjusted to scan the valid region for that initial setting. The full range of validity was explored by repetition of this process with various initial settings.

Cells and Staining

Jurkat T cells were loaded for 45 min with 10 μM Indo-1 at 37°C and washed twice with room-temperature RPMI. Measurements were made of resting cells and of samples stimulated with 2 μM Ionomycin. The PMT voltages on the Indo-1 measurement channels were adjusted so that both the resting and the stimulated populations remained as much as possible within the range of validity for the pulse-processor Lin ratio. Under this condition, data were recorded for Indo-1 violet (395–415 nm), Indo-1 green (515–560 nm), the Lin ratio, and the Log ratio. The PMT voltages were then reduced to simulate Indo-1 loading of approximately 50% and 25% of the observed level and subsequent data sets taken, respectively.

For the T cell measurements, peripheral blood mononuclear cells (PBMC) were prepared from whole blood by Ficoll density centrifugation. Washed cells were resuspended and cultured in RPMI supplemented with 10% fetal calf serum, L-glutamine, and antibiotics at a concentration of 1×10^6/ml. After 24 h at 37°C, nonadherent cells were harvested and recovered by centrifugation. Cells were resuspended in 10 ml of prewarmed medium containing 10 μM Indo-1 and incubated for 45 min at 37°C. Cells were centrifuged and resuspended at a concentration of 1×10^8/ml in RPMI containing 0.02% sodium azide at room temperature. Aliquots (200 μl) were stained for surface markers: Appropriate amounts of each antibody (FITC L-selectin, PE CD45RA, PE CD45R0, Cy5PE CD8, or Cy5PE CD4; Pharmingen, San Diego, CA) were added. After 15 min, cells were washed three times with room-temperature RPMI (with no azide). The presence of azide during the antibody staining does not affect the calcium flux. It is very important not to use chilled medium; cells cooled to 0°C had a marked deficiency in their subsequent ability to flux calcium. Cells were kept at room temperature, until 5–10 min before stimulation, at which point they were warmed to 37°C. Cells were kept at 37°C during the stimulation and FACS analysis. Cells were analyzed for 30 s prior to stimulation to collect baseline values for Indo-1 emission. The anti-CD3 antibody G19-4 (10 μg; a kind gift of Dr. J. Ledbetter, Bristol-Myers Squibb Pharmaceutical Research Institute, Seattle, WA) was added to 1 ml of cells; FACS analysis was continued for up to 15 min after this. Alternatively, 2 mM

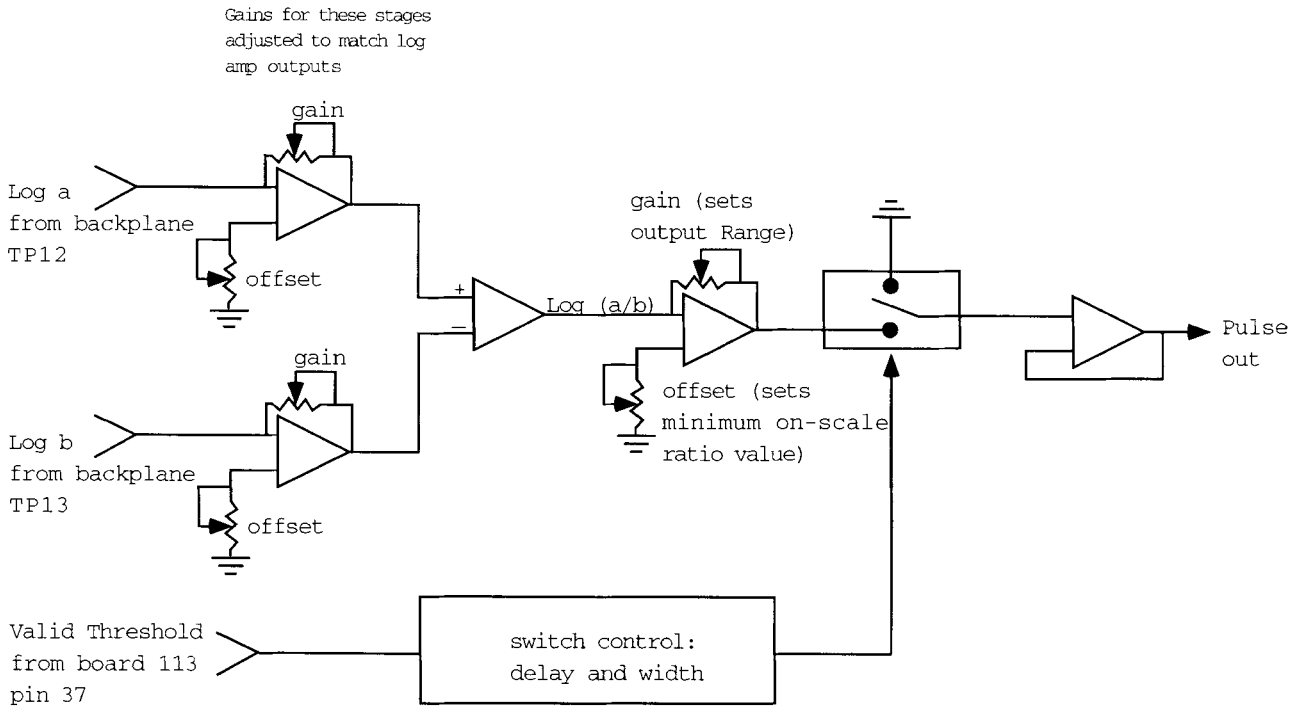

FIG. 3. Log-ratio circuit block diagram. The two held Log-signal inputs are fed through conditioning amplifiers to exactly match their characteristics and are continuously subtracted. The resulting difference signal has gain and offset to provide appropriate ratio channel scaling. An analog switch is used to form a pulse of this difference. The pulse timing and pulse width are adjustable, allowing the output to be matched with the first or second laser.

Ionomycin in DMSO was added to final concentrations as noted. The Log ratio was averaged over 10 s intervals to estimate intracellular calcium as a function of time.

RESULTS

Dynamic Range and Region of Validity Measurements

In a 3.75 decade log domain (a common range for logarithmic amplifiers), a single channel change in either of the source signals (a 3.5% step) will produce a nearly two channel change in the 2 decade Log ratio provided that everything is on scale. For this paper, we will call a ratio signal valid if a 6% change (i.e., almost two log channels) in either the numerator or the denominator produces at least an equivalent (6%) change in the ratio. The regions of validity of Indo-1 signals for both the Lin ratio and the Log ratio were determined by plotting the bead peak positions in the Indo-1 source channels, which resulted in valid ratio signals. These were obtained (see Materials and Methods) by initially setting each input channel to the ratio calculation at midscale and then independently scanning the numerator and denominator channels by adjusting the PMT voltages. Figure 4A shows the measurement data. Figure 4B summarizes the derived regions of validity. This result shows that the Lin ratio output has a dynamic range of a little over 1 decade, whereas the Log ratio provides a dynamic range of 2 decades. Moreover, the region of validity for the source signals is considerably larger for Log ratio than for Lin ratio.

The limitation on valid input signals for the Lin ratio occurs, for different reasons, in both Indo-1 signal channels. For the numerator (Indo-1 violet), the limitation is due to the linear measurement system. Given a valid denominator, the Lin ratio smoothly varies as the numerator signal level is changed. However, when the numerator is too low, the channel resolution of the resulting ratio data is insufficient to distinguish small differences in ratio. In comparison, a single channel change in either input signal in the log domain produced valid measurements across the full 2 decades of on-scale range using Log ratio. For the denominator (Indo-1 green), the Lin ratio becomes abruptly invalid below approximately the 40-signal-unit level (see Fig. 4B). This behavior is due to circuit design in which the time required to reach a stable ratio output is dependent on the denominator voltage level. When the multiplier chip has insufficient signal in the denominator, it fails to generate a correct ratio within the available evaluation time (2). This is pointed out in the pulse processor ratio adjustment procedure by the manufacturer (1). This limiting signal level can be lowered somewhat for the Becton Dickinson electronics by lengthening the evaluation dead time. However, we did observe that, within their valid ranges, both measurement systems

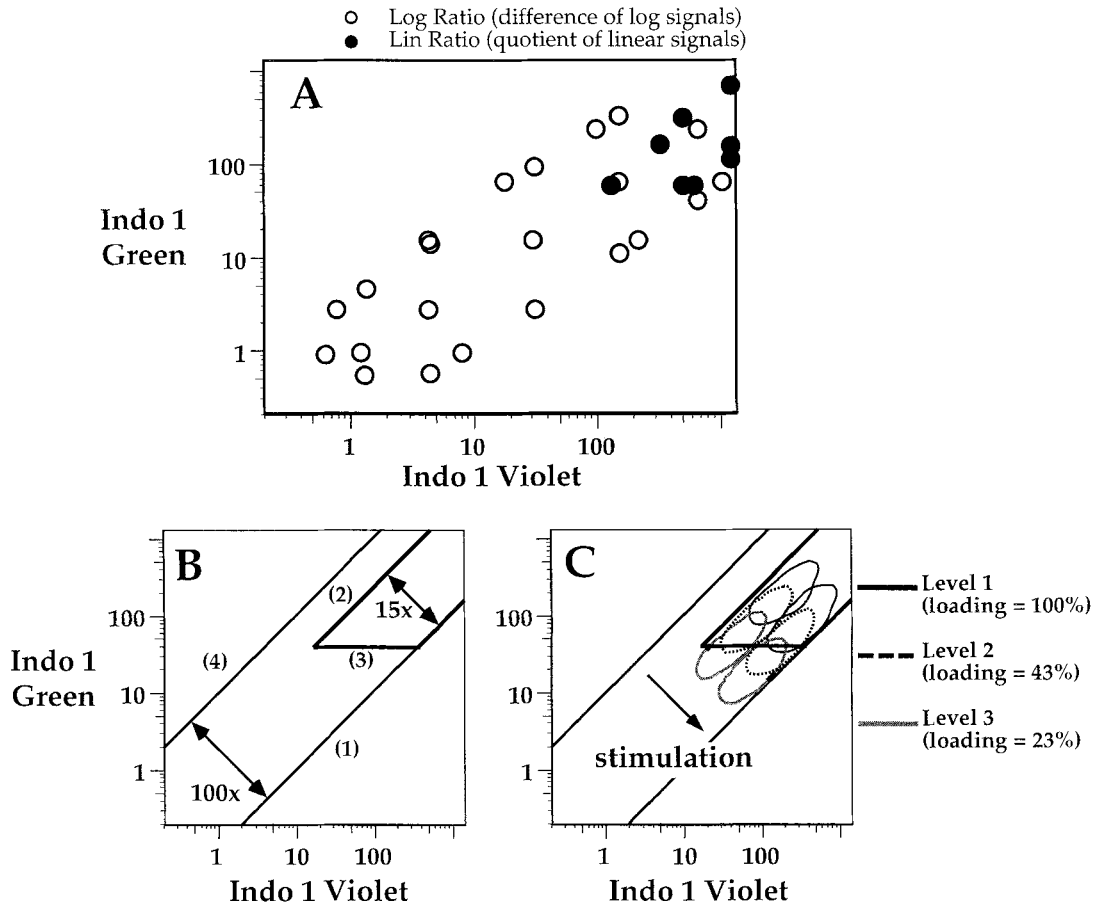

FIG. 4. Comparison of Log ratios to linear (Lin) ratios. **A:** Plot of the data obtained by varying the signal levels on beads (see Materials and Methods). Open circles are points where the Log-ratio signal is valid; solid circles are points where the pulse processed linear ratio is valid. **B:** Regions of validity for the two measurement systems based on the data in A. The Log-ratio output was adjusted to have a range of two decades, because this covers the maximal span of ratios available with Indo-1. The Log ratio is valid for all signals that fall between lines 1 and 4. The linear ratio has a range of 1:15; this is indicated by lines 1 and 2. Moreover, line 3 shows that the circuit design imposes and additional constraint on the denominator signal level (see text). **C:** Illustration of how resting and stimulated cell populations with various amounts of Indo-1 loading (default, population 1 = 100%) will fall within these ranges. The contours for each population enclose 92% of the cells. For each of the population pairs, the upper left contour represents the resting cells, and the lower right contour represents the stimulated cells. The PMT voltage for both measurement channels was adjusted to keep as much as possible of both states of population 1 on scale for linear ratio. Populations 2 and 3 were measured at this setting.

gave reasonably accurate measurements of the signal ratio (data not shown). It should be noted that the value of 40 signal units is not a "magic number." On the Becton Dickinson instrument, the log scale maps the full input signal range into 250 channels (3.75 decades), with the highest signal mapping to channel 250. The signal level at which the analog multiplier chip fails then maps to approximately 40 units on a scale of 0.2 to 1,000.

The difference in valid ranges between Lin ratio and Log ratio has clear implications for biological experiments. Figure 4C presents the results of a simulation of Indo-1 loading levels in Jurkat cells. The PMT voltages for the Indo-1 channels were adjusted to the highest values that allowed the ratios of the unstimulated and stimulated cells to remain within the range of validity of both Lin and Log ratios. Decreasing these voltage values to simulate different Indo-1 loading levels resulted in the Lin

FIG. 5. Heterogeneous calcium flux in peripheral T cell subsets after CD3 stimulation but not ionomycin stimulation. **A:** Calcium flux in the three CD4 subsets is shown as a function of time after stimulation with antibody to CD3. The naive cells have a much greater flux and maintain a greater intracellular calcium concentration for up to at least 15 min (data not shown). **B:** Five percent probability contour plots of the Indo-1 Log ratio (intracellular calcium) vs. time for each of the three CD4 subpopulations (dots represent cells lying outside of the 95% contour line). These plots show that more than 90% of all cells in each subpopulation respond to the CD3 triggering. In addition, the cells responded uniformly. Note that the raw data in B are presented as the logarithm of the Indo-1 ratio vs. linear time; the data in the line graphs (A,C) have been converted to linear. **C:** The calcium flux in these cell subsets is identical after stimulation by ionomycin. Three different concentrations of ionomycin were used to show identical responsiveness in all T cells (the three curves for each concentration are the responses by the naive, M1, and M2 CD4 T cells shown in Fig. 6).

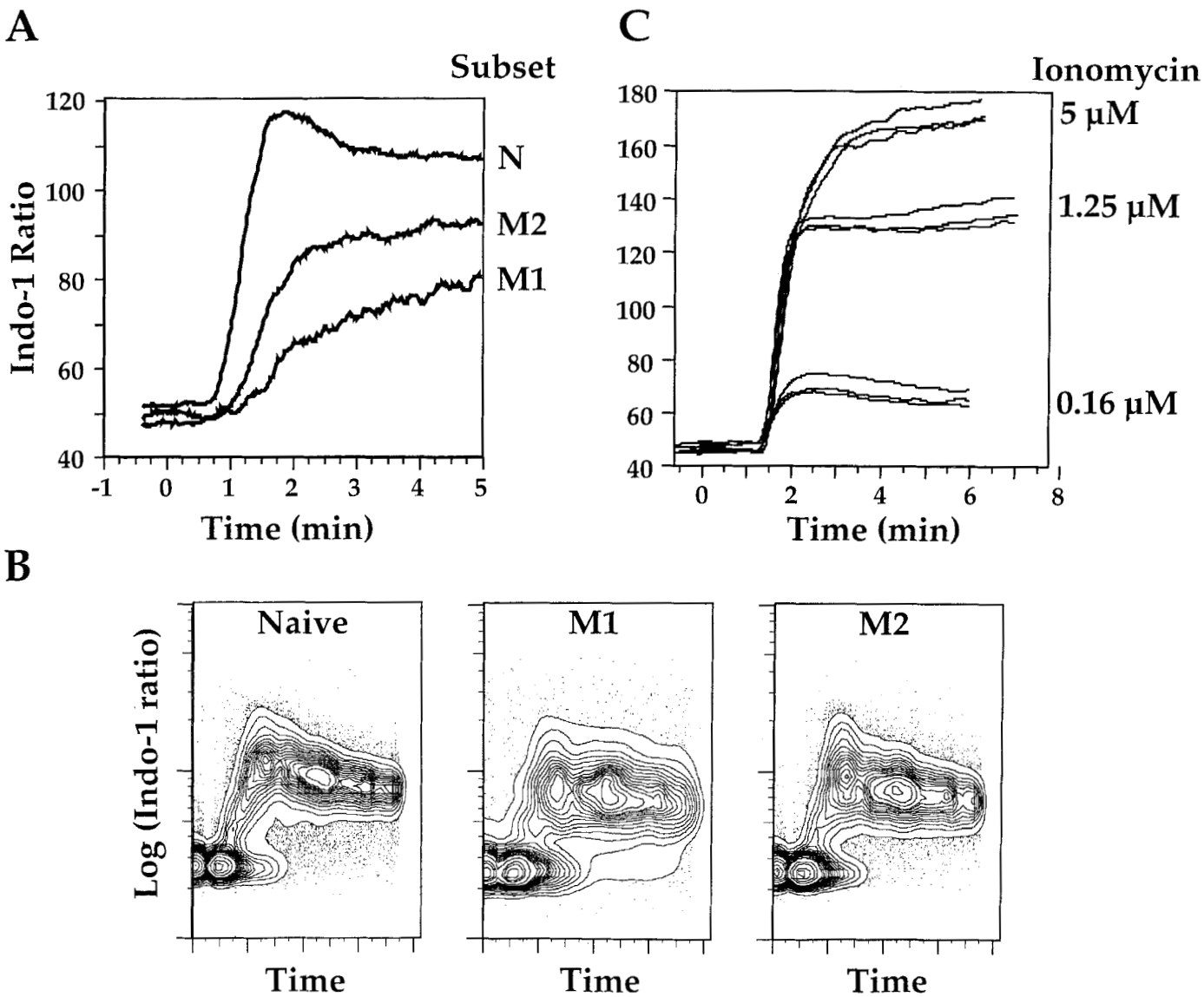

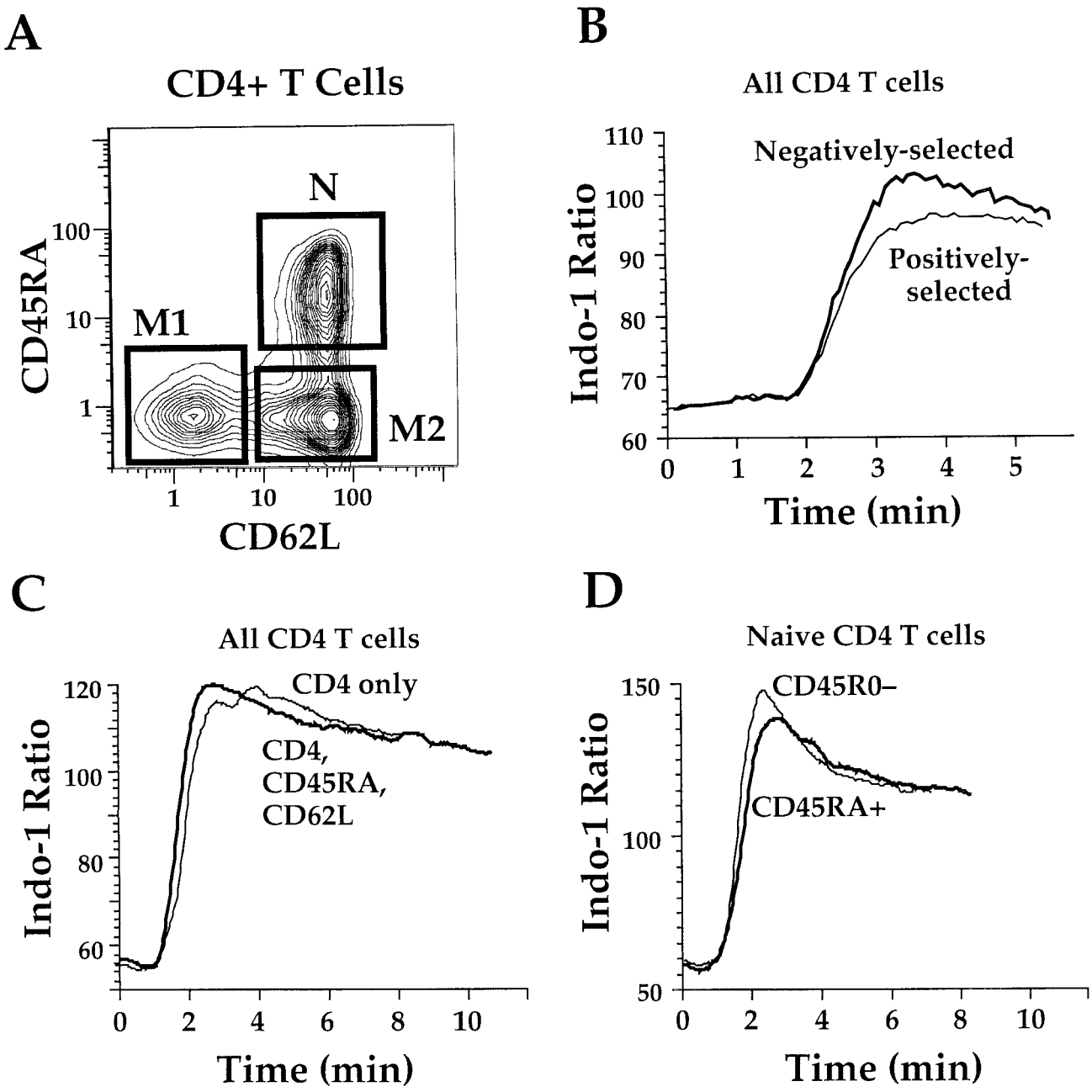

FIG. 6. Surface immunofluorescence staining methodology does not affect calcium flux. **A:** CD4 T cells (defined using a forward scatter for lymphocytes and a $CD4^+$ fluorescence gate) can be subdivided into three subpopulations based on the expression of CD45RA and CD62L. The double-positive population (N) contains naive cells, which are defined as cells that do not respond to recall antigen. The other two populations (M1 and M2) are memory populations. Controls (B–D) were performed to demonstrate that the antibody staining procedure (i.e., presence of antibodies on the surface of the cells) does not alter the calcium flux induced by anti-CD3. **B:** CD4 T cells were identified either by the presence of anti-CD4 (positively selected) or by the absence of anti-CD8, anti-CD56, and anti-CD20 (negatively selected). Thus, the negatively selected cells have no surface antibody bound at the time of addition of anti-CD3. The calcium flux for these cells is virtually identical (in five experiments) to that for cells that had anti-CD4 bound. **C:** Calcium flux for all CD4 T cells was compared in cells stained with only CD4 and cells stained with CD4, CD45RA, and CD62L. Again, the cells showed identical fluxes, demonstrating that the CD45RA and CD62L binding had a minimal effect on the response to anti-CD3. **D:** Cells were stained either with CD4 and CD45RA or with CD4 and CD45R0. The $CD45RA^+$ cells are equivalent to the $CD45R0^-$ cells and vice versa. In this graph, the calcium flux of the naive cells ($CD45RA^+$ or $CD45R0^-$) was independent of the antibodies used. This proves definitively that the binding of CD45RA antibodies did not affect the distribution of the calcium flux in these cells. The calcium flux in the memory populations ($CD45RA^-$ or $CD45R0^+$) was similarly unaffected by the binding of the CD45R0 antibody (data not shown).

ratio becoming invalid (indicated by going to the top or bottom of the measurement scale), whereas the Log ratio remained measurable (Fig. 4C). Thus, although it is possible to adjust the source signal levels to obtain a valid Lin ratio measurement for most single Indo-1 samples, there may be no single configuration that will yield valid measurements of multiple samples with different amounts of dye loading or of single samples with particularly heterogeneous Indo-1 levels. This limits experiments whose analyses depend on a comparison of relative ratios over time or between samples. The use of Log ratios will minimize or eliminate this problem.

Calcium Flux in T Cell Subsets

Figure 5A shows that phenotypically distinct subsets of CD4 T cells have very different profiles of calcium flux after anti-CD3 stimulation. Naive CD4 T cells, ($CD45RA^+$, $CD62L^+$; see Fig. 6A), have the strongest flux. Although the kinetics for all the populations are roughly the same, naive cells show the greatest peak concentration of calcium as well as the highest resulting "steady-state" level. The two memory populations, distinguished by L-selectin (CD62L) expression, also have distinct calcium flux capacities; the $CD45RA^-$ $CD62L^-$ population has the weakest flux. The subset difference in the ability to flux calcium is also true at suboptimal doses of anti-CD3 (data not shown). The response to the anti-CD3 trigger was quite uniform, in that virtually all cells responded (Fig. 5B). In addition, within a subset, the response was similar for all cells (i.e., at any point in time, the distribution of intracellular calcium concentrations was roughly log normal).

This difference in response was specific to antigen receptor (anti-CD3) triggering; i.e., cells from all three subsets had indistinguishable calcium flux responses after triggering by ionomycin (Fig. 5C). This suggests that there was no difference between the subsets in the mechanisms responsible for transporting calcium (either in the endoplasmic reticulum, where ionomycin generates the small calcium flux trigger, or at the cell membrane, where a majority of calcium is transported). Therefore, the difference observed after anti-CD3 triggering reflects a difference in the signal transduction pathways within these subsets.

Incubation of cells with specific antibodies to certain receptors often can alter the cells' responsiveness. Thus, it is important to ascertain whether the difference in calcium flux by the subpopulations is a functional difference or if it is due to the differential binding of antibodies to the surface of these cells. For instance, it is possible that the combination of L-selectin and CD45RA antibody binding, which is used to identify the naive subset, significantly boosts the signaling transduced through the CD3 receptor.

Several controls demonstrate that, under our staining conditions, the CD45RA and L-selectin antibodies do not significantly alter the calcium flux. 1) Aliquots of the same cells were stained with only CD4. The total CD4 calcium flux (i.e., the calcium flux averaged over all CD4 T cells) of these cells was compared to cells stained with all three antibodies: There was no significant difference (Fig. 6C). This suggests, but does not directly prove, that the staining does not alter the calcium flux. It is still possible, though unlikely, that the addition of the antibodies increases the flux of some cells and decreases the flux of other cells, such that the average flux for all cells is equivalent. 2) Aliquots were stained with Cy5PE CD8, CD20, and CD56 with or without the FITC L-selectin and PE CD45RA. The calcium flux of the $Cy5PE^-$ cells (of which more than 95% are CD4 T cells) was unaffected by the L-selectin and CD45RA stains and was similar to the positively identified Cy5PE CD4 cells (Fig. 6B). This proves directly that the CD4 antibody itself does not alter the induced calcium flux. 3) Aliquots were stained with CD45R0 instead of CD45RA: These two antibodies stain mutually exclusive resting peripheral T cell subsets. Again, the $CD45R0^-$ cells showed the same calcium flux as $CD45RA^+$ cells (Fig. 6D) and vice versa, proving that the CD45RA/R0 staining does not alter the calcium flux. Together, these data prove that surface staining can be accomplished with at least some markers without affecting subsequent calcium flux.

Similar experiments were performed on CD8 subpopulations (9). As was the case for CD4 T cells, naive ($CD62L^+$ $CD45RA^+$) CD8 T cells had the greatest peak and sustained calcium concentration after stimulation. The various memory subsets had uniformly less flux, similar to CD4 T cells. Unlike CD4 T cells, CD8 T cells have a third memory subset ($CD62L^-$ $CD45RA^+$); the calcium response in this subset was essentially absent (9).

DISCUSSION

The desirable characteristics of the ratio of two signals include ranges on both the input signals and the output ratio sufficient to measure relevant biological changes as well as to sort. The approach used in the majority of commercial instruments, called Lin ratio, uses the analog quotient of the two raw signals. We have shown that this method significantly restricts the dynamic range of the input signals and scaling of the output ratio. We demonstrate a method using the difference of the logs of the raw signals to calculate the log of the ratio of the signals. This approach allows us to define one standard setup for the cytometer (PMT voltages and channel gains) for measuring Indo-1. Using this setup, the primary Indo-1 signals as well as the derived ratio signal will be on scale for almost all cells regardless of dye loading or other sample-to-sample or experiment-to-experiment variation.

Current commercial systems do not support sorting on the difference of two signals (e.g., sorting on the relative calcium concentration). The methodology described here provides a real-time signal to the instrument on which sort decisions can be made. This allows the use of rectangular gates to sort cells based (for instance) on intracellular calcium levels. Indeed, we have successfully sorted cells with altered calcium flux responsiveness by using the calcium channel as a sort decision gate.

There is a caveat in using Log ratios instead of Lin ratios. The linear amplifiers used in flow cytometry are generally quite linear over their signal range. Thus, the accuracy of the Lin ratio depends on the linearity of the division circuit used. However, a logarithmic amplifier is rarely truly logarithmic over its entire range (7). This will translate into errors in the Log ratio when comparing the two ratio values. The magnitude of this error depends on the relative deviations of the two input log signals. On the FacstarPlus, our measurements indicate that the ratio deviations are less than 5% over a full decade range (data not shown).

Previous studies have identified heterogeneous calcium flux responses in phenotypically distinct T cell subpopulations. Rabinovitch et al. (10) demonstrated that, after phytohemagglutinin (PHA) stimulation, human CD4 T cells had a stronger response than CD8 T cells. In addition, the authors showed that subsets discriminated only by CD45 isoforms had mildly distinct fluxes. The greater differences shown in this report are probably due to a finer discrimination of functionally distinct subsets. In addition, Nagelkerken and Hertogh-Huijbregts (5) used two-color immunofluorescence phenotyping to show that memory T cells in mice had a considerably lesser ability to flux calcium than naive T cells. These investigators also demonstrated that this differential response was specific to CD3 triggering.

The requirement for more and more independent "colors" to distinguish T cell subsets is continually increasing. At least three distinct subsets of CD4 T cells and four distinct subsets CD8 T cells can be identified on the basis of CD62L and CD45RA. One of each of these is "naive"; the remainder are "memory" populations. These populations are functionally distinct; in vitro, they have significantly different capacities to flux calcium in response to CD3 triggering, as we have shown here. In addition, these different subsets have significantly different cytokine profiles (9). This difference is not simply along the naive-memory division; phenotypically distinct memory subsets also show significantly different capacities to flux calcium. It might be predicted from the calcium flux that their proliferative capacity in response to various stimuli is also variable, with the naive cells, in general, proliferating the best (9).

There is a very significant alteration in the representation of these subsets in the blood in some pathogenic conditions. For instance, in HIV-infected people, there is an almost complete loss of the naive cells (9,11). Based on studies like the one presented here, we can predict that the functionality of PBMC from human immunodeficiency virus (HIV)-infected people will be significantly different from that of PBMC from healthy people, because there is a significantly different representation of functionally distinct subpopulations. To understand fully the profound changes in the functionality of the immune system in diseases such as acquired immunodeficiency syndrome (AIDS), we must first understand the functional capacity of the various subsets present. In this way, we can distinguish the difference in functionality due to altered representation from change in the functional capacity of individual cells. Such knowledge will have direct bearing on our understanding of the pathogenesis of HIV and on avenues of treatment of the disease.

ACKNOWLEDGMENTS

The authors thank Mr. Stote Ellsworth, formerly of Becton Dickinson Immunocytometry Systems, for his cooperation in supplying us with information regarding the FacstarPlus and the mysteries of pulse processor register settings. We thank Dr. Terry Kavanagh for suggestions on the staining protocol for calcium flux and Dr. Michael Anderson for advice. We also thank Mr. Robert Auer of Coulter Corporation for discussion of Coulter's implementation of linear ratios. M.R. is a Senior Fellow of the Leukemia Society of America.

LITERATURE CITED

1. Becton Dickinson Immunocytometry Systems: User Guide for the FacstarPlus Pulse Processor (11-10481-99 Rev A), 1988.
2. Analog Devices. In: Linear Products Databook. Norwood, MA, 1988, pp 6-13–6-30.
3. Loken MR, Parks DR, Herzenberg LA: Two-color immunofluorescence using a fluorescence-activated cell sorter. J Histochem Cytochem 25:899–907, 1977.
4. Moore WA, Kautz RA: Data analysis in flow cytometry. In: Handbook of Experimental Immunology, 4th Ed, Weir DM, Herzenberg LA, Blackwell C, Herzenberg LA (eds). Blackwell Scientific Publications, Oxford, 1986, pp 30.1–30.11.
5. Nagelkerken L, Hertogh-Huijbregts A: The acquisition of a memory phenotype by murine $CD4^+$ T cells is accompanied by a loss in their capacity to increase intracellular calcium. Dev Immunol 3:25–34, 1992.
6. Okumura M, Fujii Y, Inada K, Nakahara K, Matsuda H: Both $CD45RA^+$ and $CD45RA^-$ subpopulations of $CD8^+$ T cells contain cells with high levels of lymphocyte function-associated antigen-1 expression, a phenotype of primed T cells. J Immunol 150:429–437, 1993.
7. Parks DR, Bigos M, Moore WA: Logarithmic amplifier transfer function evaluation and procedures for Log Amp optimization and data correction. Cytometry Suppl 2:27, 1988.
8. Picker LJ, Treer JR, Ferguson DB, Collins PA, Buck D, Terstappen LW: Control of lymphocyte recirculation in man. I. Differential regulation of the peripheral lymph node homing receptor L-selection on T cells during the virgin to memory cell transition. J Immunol 150: 1105–1121, 1993.
9. Rabin RL, Roederer M, Maldonado Y, Petru A, Herzenberg LA, Herzenberg LA: Altered representation of naive and memory CD8 T cell subsets in HIV-infected children. J Clin Invest 95:2054–2060, 1995.
10. Rabinovitch PS, June CH, Grossmann A, Ledbetter JA: Heterogeneity among T cells in intracellular free calcium responses after mitogen stimulation with PHA or anti-CD3: Simultaneous use of indo-1 and immunofluorescence with flow cytometry. J Immunol 137:952–961, 1986.
11. Roederer M, Dubs JG, Anderson MT, Raju PA, Herzenberg LA, Herzenberg LA: CD8 naive T cell counts decrease progressively in HIV-infected adults. J Clin Invest 95:2061–2066, 1995.
12. Tsien R: Fluorescent indicators of ion concentrations. In: Methods in Cell Biology, Taylor DL, Wang Y-L (eds). Academic Press, New York, 1989, pp 127–156.